DISCOVERING PROTOSTARS AND THEIR HOST CLUSTERS VIA WISE

D. Majaess
Halifax, Nova Scotia, Canada.
dmajaess@cygnus.smu.ca

ABSTRACT

A hybrid $JHK_s - W_1W_2W_3W_4$ high-spectral index (α) selection scheme was employed to identify (sub)clusters of class I/f candidate protostars (YSOs) in WISE observations (the Wide-Field Infrared Survey Explorer). $n > 10^4$ candidate YSOs were detected owing to WISE's advantageous all-sky spatial coverage, and a subsample ($n \sim 200$) of their heavily-obscured host (sub)clusters were correlated with the Avedisova (2002) and Dias et al. (2002) catalogs of star-forming regions. Forthcoming observations from the VVV/UKIDSS surveys shall facilitate the detection of additional protostars and bolster efforts to delineate the Galactic plane, since the campaigns aim to secure deep JHK_s photometry for a pertinent fraction of the WISE targets lacking 2MASS detections, and to provide improved data for YSOs near the limits of the 2MASS survey.

Subject headings: circumstellar matter, infrared: stars, stars: formation

1. INTRODUCTION

Identifying young stellar objects (YSOs) and their host clusters bolsters efforts to constrain the star formation rate, local starburst history (Bonatto & Bica 2011, their Fig. 1), cluster dissolution timescale ('infant mortality rate' for protoclusters, Lada & Lada 2003), and the Galaxy's spiral structure. Bonatto & Bica (2011) examined newly identified clusters (e.g., Bica et al. 2003) and inferred that the local star formation rate is not constant and is punctuated for $\tau \leq 9$ and 220-600 Myr, while Spitzer legacy results for five nearby protostar-hosting complexes imply that a sizable fraction of the YSOs lie in loose clusters ($n > 35$, $\rho > 1 M_{\odot}/\mathrm{pc}^3$, Evans et al. 2009). Such pertinent determinations may be invariably strengthened by increasing the statistics of known protostars and protoclusters. Hence the importance of infrared surveys such as WISE (Wright et al. 2010), which facilitate the discovery of such objects (Liu et al. 2011; Rebull et al. 2011; Majaess et al. 2012; Koenig et al. 2012).

Historically, new Galactic clusters were often identified while inspecting photographic plates imaged near optical wavelengths. Young embedded clusters were consequently under-sampled since dust extinction is wavelength-dependent. By comparison to optical observations, infrared photometry suffers an order of magnitude less dust obscuration (e.g., $A_{[4.5\mu m]} \sim 0.05 A_V$, Flaherty et al. 2007). Forthcoming results from the VVV/UKIDSS *near*-infrared surveys (Lucas et al. 2008; Minniti et al. 2010) are thus pertinent for detecting YSOs and their host clusters, and the observations will extend $\sim 4^{\mathrm{m}}$ fainter than 2MASS for Galactic disk stars. The VVV survey shall establish precise multi-epoch JHK_s photometry for fields in the Galactic bulge and near the Galactic plane ($\ell, |b| \sim 294.7, 350.0 : 2.3^{\circ}$ & $\ell, b = 350.0, 10.4 : -10.3, 5.1^{\circ}$, Minniti et al. 2010; Catelan et al. 2011). WISE images exhibit a marked improvement in resolution and sensitivity over existing *mid*-infrared surveys (e.g., IRAS), and sample the sky at 3.4 (W_1), 4.6 (W_2), 12 (W_3), and 22 μm (W_4). The corresponding FWHM are $6.1''$ (W_1), $6.4''$ (W_2), $6.5''$ (W_3), and $12.0''$ (W_4). The Spitzer GLIMPSE surveys (Galactic Legacy Infrared Mid-Plane Survey Extraordinaire, Benjamin et al. 2003; Churchwell et al. 2009) feature superior resolution relative to WISE, however WISE provides increased (all-sky) coverage. Extending the GLIMPSE surveys to encompass broader regions of the Galaxy is consequently desirable, and forthcoming.[1]

The latest generation of infrared surveys are aptly tailored to detect YSOs and their host environments. Robitaille et al. (2008), Evans et al. (2009), and Gutermuth et al. (2010) used Spitzer data to classify $> 13 \times 10^3$ YSOs. Borissova et al. (2011) discovered 96 candidate clusters[2] in the VVV survey (Minniti et al. 2010), while Mercer et al. (2005) identified 92 star clusters via GLIMPSE data (see also Froebrich et al. 2007; Kronberger et al. 2006). Those infrared surveys resolved numerous individual cluster stars, and in many instances confirmed existing evidence of star formation put forth by low-resolution surveys (e.g., IRAS and maser observations, Avedisova 2002). The term discovery is hence somewhat subjective, since a sizable fraction

[1] `http://www.astro.wisc.edu/glimpse/`

[2] Chené et al. (2012) discovered numerous Wolf-Rayet stars residing in those clusters using infrared spectra from the VLT, NTT, and SOAR facilities.

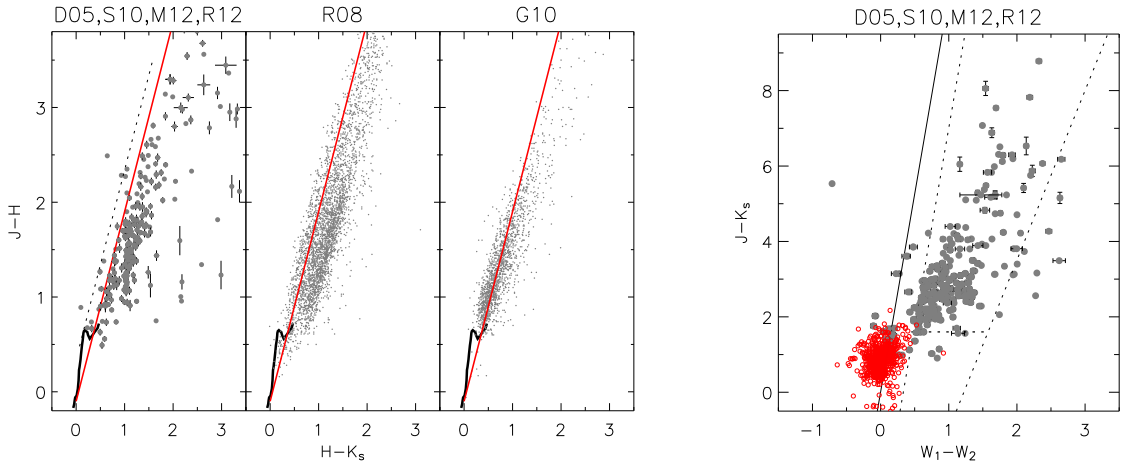

Fig. 1.— Left, JHK_s color-color diagrams featuring YSO candidates identified by Doppmann et al. (2005, D05), Robitaille et al. (2008, R08), Gutermuth et al. (2010, G10), Straižys & Kazlauskas (2010, S10), Majaess et al. (2012, M12), and Rosvick (2012, in prep, R12). The canonical JHK_s reddening law established by Straižys & Laugalys (2008) and Majaess et al. (2011) was adopted. The black line is the intrinsic relation for main-sequence dwarfs (Straižys & Lazauskaitė 2009), while the dashed line defines the reddening trajectory for red clump stars (Straižys & Laugalys 2008; Majaess et al. 2011). The YSOs lie principally redward of the solid (red) line, and thus that will be adopted as a boundary condition for identifying YSO candidates in the present analysis. Right, $JK_sW_1W_2$ color-color diagram featuring the YSO samples of D05, S10, M12, and R12. The YSOs are located primarily within the region bounded by the dashed lines, which will likewise be adopted as boundary conditions for identifying YSO candidates. The solid line represents the approximate reddening vector for earlier-type stars, while the open red circles define field stars, which typically do not display the signature of IR-excess. To avoid cluttering the diagrams, errors bars are shown for a subset of the data possessing uncertainties.

of the aforementioned identifications exhibit entries in the Avedisova (2002) catalog of star-forming regions, and indeed that is likewise true of the targets described in §2.3.

In this study, a hybrid $JHK_s - W_1W_2W_3W_4$ high-spectral index (α) selection scheme is used to identify YSOs and their host complexes. This paper is organized as follows: in §2.1.1 2MASS/WISE color-color cuts inferred from known YSOs, in concert with the slope (α) of the spectral energy distribution (SED, §2.1.2), is used to identify YSO candidates (§2.2); in §2.3 numerous (sub)clusters hosting the detected YSOs are tabulated, whereby subclusters are offshoot clumps of emerging stars tied to broader star-forming regions (hierarchical clustering); in §2.4 the pertinence of the VVV/UKIDSS surveys for expanding the YSO sample size is described; and the results are summarized in §3. A detailed characterization of individual YSOs (SED modelling, Robitaille et al. 2007) and protoclusters shall await additional observations (e.g., ALMA), and will be pursued elsewhere. Ultimately, the results will bolster the statistics linked to supporting new theories of star-formation (e.g., the 'fireworks hypothesis', Koenig et al. 2012), and constraining parameters such as the star formation rate and local starburst history (e.g., Bonatto & Bica 2011).

2. ANALYSIS

2.1. YSO SELECTION SCHEME

2.1.1. $JHK_sW_1W_2$ CRITERIA

A JHK_s color-color diagram (Fig. 1) is compiled for the YSO candidates highlighted by Doppmann et al. (2005), Robitaille et al. (2008), Gutermuth et al. (2010), Straižys & Kazlauskas (2010), Majaess et al. (2012), and Rosvick et al. (2012, in prep)[3].

Fig. 1 reaffirms that the least evolved YSOs typically occupy positions redward ($H-K_s$) of the reddening line defined by red clump and OB stars. A fraction of the candidates in Fig. 1 lie within the region tied to reddened stars rather than those exhibiting strong infrared excess. Uncertainties tied to individual passbands add in quadrature and complicate the analysis. The resulting color-color uncertainties are particularly onerous and can be underestimated for YSOs, which occupy complex encironments and can be detected near the 2MASS survey limits owing to sizable extinction. The pertinence of the VVV survey for alleviating that problem is discussed

[3]Rosvick et al. (2012, in prep) detail a new YSO subcluster discovered in JHK_s images acquired from l'Observatoire Mont-Mégantic (OMM, Artigau et al. 2010). The group was likely triggered by adjacent luminous O-type stars in Berkeley 59 (e.g., the O5V((f))n BD+64°1673, Majaess et al. 2008, see also Koenig et al. 2012). The Doppmann et al. (2005) results are tied to high-resolution infrared Keck spectra for 41 class I/f YSOs.

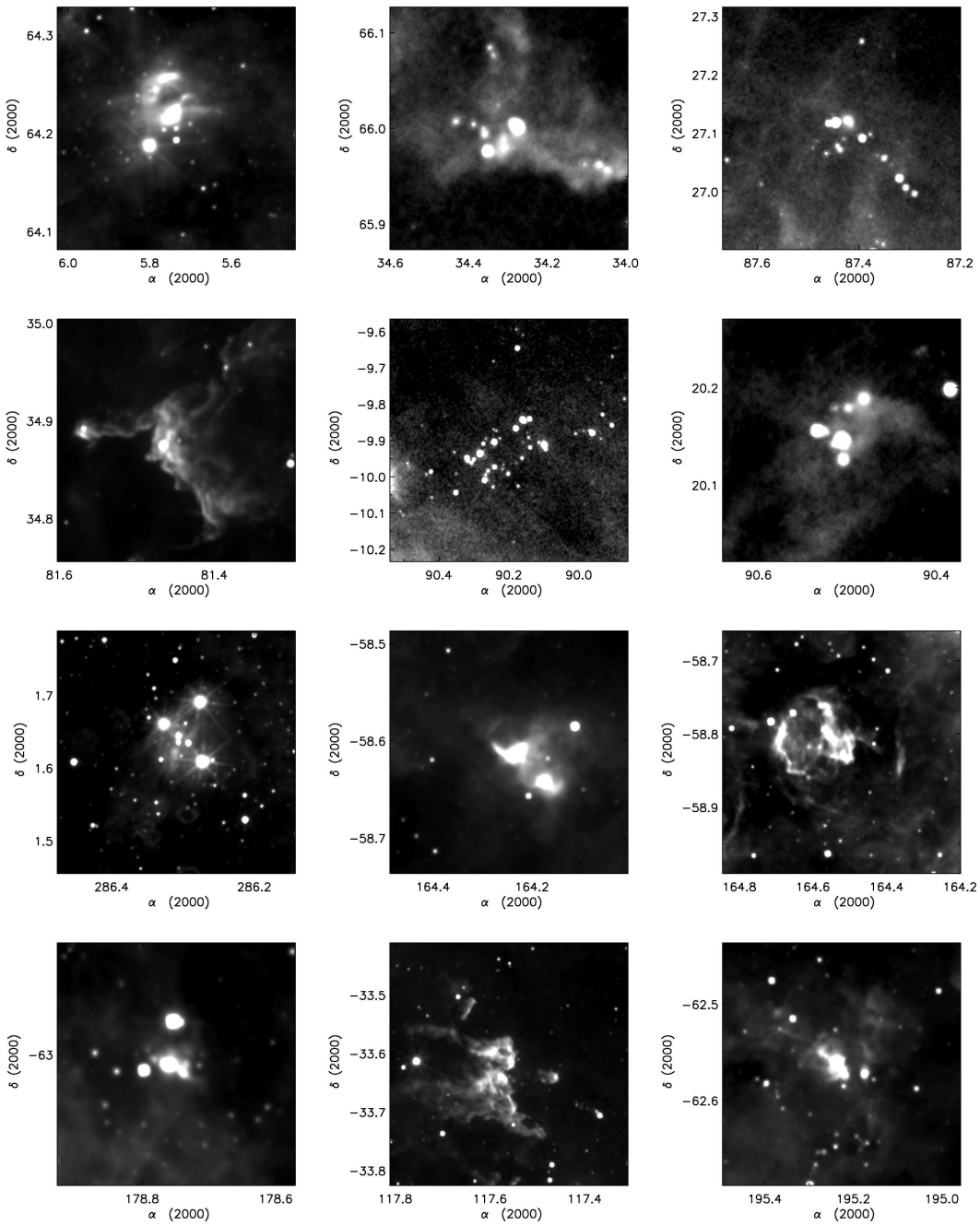

Fig. 2.— WISE images for a subset of the obscured (sub)clusters detailed in Table 1.

in §2.4, since the survey extends deeper than 2MASS and exhibits reduced uncertainties for fainter stars. A photometric cut may be adopted to mitigate field contamination by requiring that relatively unevolved YSOs lie redward of the reddening line for red clump and OB stars, i.e. $(J-H) < E(J-H)/E(H-K_s) \times (H-K_s) - 0.15$ and $(J-H) > 1$. WISE data (W_1W_2) may be employed to extend the wavelength baseline and facilitate the detection of infrared excess. The YSOs identified by Doppmann et al. (2005), Straižys & Kazlauskas (2010), Majaess et al. (2012), and Rosvick (2012, in prep) occupy a $JHK_sW_1W_2$ color-color region separated from reddened stars (Fig. 1). The following color selection scheme approximately defines that region: $(J-K_s) < 10.5 \times (W_1-W_2) - 3.5$, $(J-K_s) > 4.5 \times (W_1-W_2) - 5.5$, and $(J-K_s) > 1.6$. Field stars typically do not fall into that regime (Fig. 1, red open circles). A comparison of low and high-latitude objects passing the aforementioned criteria implies that a magnitude cutoff ($W_3 < 8.7$) reduces contamination by galaxies at larger latitudes.

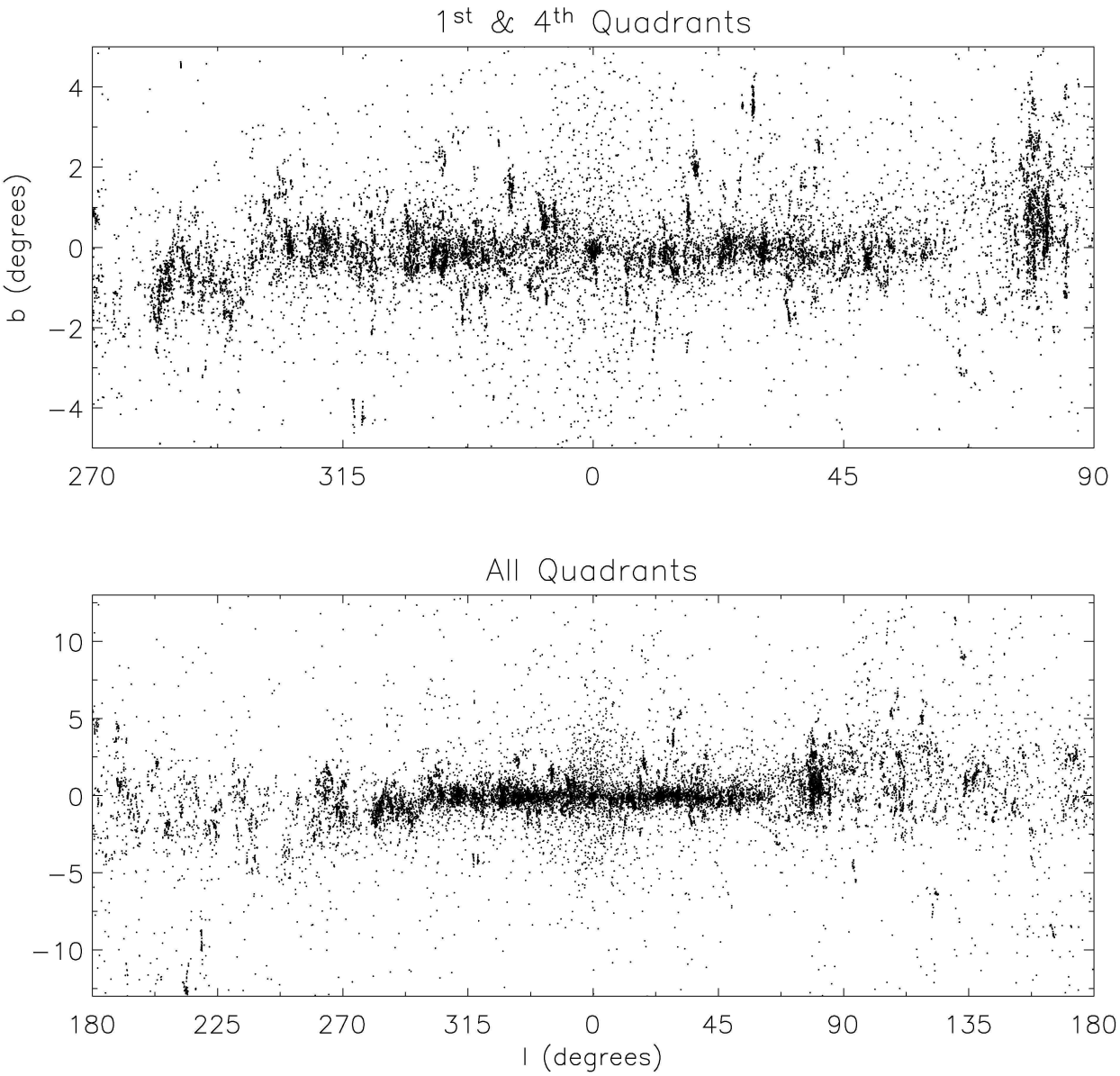

Fig. 3.— Delineation of the Milky Way via the YSO candidates identified. Large star-forming regions and the warp induced in part by the LMC are discernible.

2.1.2. α CRITERION

The slope of the SED (spectral index α) may be used to facilitate the classification of YSOs. The canonical framework defines class I, flat, class II, and class III YSOs as featuring $\alpha > 0.3$, $-0.3 < \alpha < 0.3$, $-0.3 > \alpha > -1.6$, and $\alpha < -1.6$ respectively (Greene et al. 1994, see also Evans et al. 2009). However, the wavelength dependence of extinction, in concert with a given YSO's inclination/orientation, introduce degeneracies. Radiation emitted at 2MASS K_s exhibits increased sensitivity to extinction compared to WISE passbands (Flaherty et al. 2007). α is thus sensitive to extinction, and reddened stars may be misclassified as younger protostars (Majaess et al. 2012, see also §7.2 in Evans et al. 2009 and their discussion concerning the Ophiuchus cloud). Consequently, the spectral index is often employed in tandem with color-color analyses to identify YSOs (e.g., Gutermuth et al. 2010; Majaess et al. 2012).

Field contamination may be reduced by assessing the positions of high-spectral index candidates in color-color diagrams (Fig. 1). High spectral index objects were identified by evaluating the slope of the $\log(\lambda F_\lambda)$ function via least-squares (LS) and robust (R) fitting routines. The fitting routines yield comparable slopes when using 2MASS K_s+ WISE photometry, but deviate when relying solely on WISE photometry. The deduced spectral index is sensitive to the fitting routine and passbands used, and the topic is worth elaborating upon in a separate work (the systematics are not deleterious for the present analysis). Alternatively, α may be inferred directly from the WISE photometric colors, which is beneficial when 2MASS photometry isn't available: $\alpha_{(LS,W,p)} \sim 0.36(W_1-W_2)+0.58(W_2-W_3)+0.41(W_3-W_4)-2.90$. Only targets with S/N> 5 in all WISE passbands were examined, as longer-wavelength 22 μm data are valuable for culling non-YSO contaminants (see also Robitaille et al. 2008). $\sim$ 20% of the YSO candidates identified toward the Serpens cloud may be reddened giants masquerading as class II/III sources (Evans et al. 2009, and references therein).

To minimize field contamination (e.g., AGB stars) only class I/f objects ($\alpha > -0.3$, §2.1.2) are henceforth examined. Highly reddened field stars (e.g., giants) may exhibit values of α similar to class II/III objects, and indeed, the majority of the AGB stars highlighted by Robitaille et al. (2008) peak near $\alpha \sim -0.9$. Conversely, the YSOs identified by Robitaille et al. (2008) peak near $\alpha_{(LS,W,p)} \sim -0.1$.

2.2. YSO CANDIDATES

High spectral index stars matching the aforementioned $JHK_sW_1W_2W_3W_4$ criteria are classified as YSO candidates. $\sim 10 \times 10^3$ class I/f YSOs were identified in the VVV survey area, and 30×10^3 objects throughout the WISE survey. The identification of a YSO may be spurious owing to field contamination, photometric uncertainties and blending/crowding (multiple sources falling within the FWHM). Field contamination appears reduced since < 10% of the AGB stars identified by Robitaille et al. (2008) were classified as YSO candidates via the present hybrid selection scheme. Robitaille et al. (2008) did not assess YSOs with close neighbors (Fig. 2) in order to mitigate crowding/blending, and adopt $\alpha > -1.2$ as a threshold to detect class II objects. Only class I/f YSOs were assessed here to reduce field star contamination and an objective was to examine (crowded) protoclusters (Fig. 2). Admittedly, the criteria adopted here are exceedingly conservative for analyzing obvious YSOs (e.g., class II) in clusters (Fig. 2), and too lax for objects at large Galactic latitudes (b) where field contamination (i.e., galaxies) is acute. Photometric contamination from (non) stellar sources associated with the environment surrounding YSOs will affect the WISE data analyzed, owing in part to the reduced spatial resolution of the observations relative to 2MASS and the matching of the detected sources. Yet a close-neighbor rejection criterion was avoided in order to achieve the objective of detecting compact groups of YSOs. Approximately 90% of the YSOs identified lack 2MASS neighbors within half the FWHM of the shorter-wavelength WISE passbands. However, higher-resolution Spitzer photometry via an expansion of the GLIMPSE surveys is desirable.

2.3. YSO COMPLEXES

The class I/f YSO candidates identified delineate the Galactic plane as expected (for a comparison to the older PNe distribution see Majaess 2010). The ascent from negative b ($\ell \sim 270-300^\circ$ to $\ell \sim 90^\circ$) is likewise observed in the distribution of classical Cepheids (Majaess et al. 2009, see also the Dame et al. 2001 CO survey). Distinct conglomerates containing sizable numbers of YSOs are discernible in Fig. 3 (e.g., $\ell, b \sim 19, 2^\circ$). A subsample of the embedded clusters identified, with an emphasis on smaller overlooked subclusters (see also Koenig et al. 2012), are highlighted in Table 1 and Fig. 2. The objects are typically not discernible in optical and even 3.4 μm images, which underscores the extreme obscuration. The bulk of the targets deviate from spherical symmetry and are typically associated with larger complexes (hierarchical clustering). Constituent stars are observed to emerge from dusty filamentary structure and at the periphery of bubbles (see also Koenig et al. 2012). The objects were identified while visually inspecting the distribution of YSO candidates (Fig. 3) using the Aladin software environment (Bonnarel et al. 2000). Apparent sizes for the (sub)clusters are outlined in Table 1, and those targets tagged by an asterisk contain few members. The majority of the targets will dissolve prior to achieving open cluster status (Lada & Lada 2003). In many instances the objects are near IRAS and maser sources tabulated in the catalog of star-forming regions (Avedisova 2002). The nearest (projected separation)

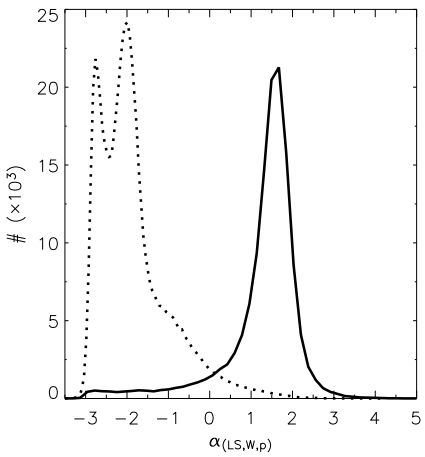

Fig. 4.— The spectral index ($\alpha_{(LS,W,p)}$) distribution for WISE targets (S/N> 5) featured in the VVV region (dashed-line). Stars associated with the maxima exhibit JHK_s colors indicative of late-type giants. The distribution (solid-line) for $> 10^5$ stars ($|b| < 10^\circ$) lacking 2MASS photometry lies principally beyond $\alpha_{(LS,W,p)} > 0.3$ (potentially class I YSOs), hence the pertinence of the forthcoming VVV/UKIDSS results (§2.4).

star-forming region lying $r < 30'$ is listed in Table 1, and the offsets between the objects are tabulated. The (sub)clusters identified were likewise correlated with the Dias et al. (2002) catalog. The nearest young clusters ($r < 20'$) are listed in Table 1. The aforementioned catalog is regularly updated, however, the (sub)clusters may be tabulated elsewhere in which case the class I/f YSO members identified here may confirm existing classifications and place solid constraints on the age of the host clusters ($10^5 - 10^6$ yr). Clusters which were identified serendipitously as a result of the analysis are likewise tabulated. Table 1 shall be made available online in the DAML and WEBDA catalogs (Dias et al. 2002; Paunzen 2008), as the vast majority of the targets highlighted do not exhibit counterparts in those catalogs.

2.4. PERTINENCE OF THE VVV/UKIDSS SURVEYS

A fraction of the class I YSOs identified by Majaess et al. (2012) in the star-forming complex near the classical Cepheid SU Cas lacked 2MASS detections. Indeed, $> 10^5$ objects ($|b| < 10^\circ$, $W_3 < 8.7$) featuring S/N> 5 in all WISE passbands lack 2MASS photometry. That sample lies principally beyond $\alpha_{(LS,W,p)} > 0.3$ (class I, Fig. 4). One of the main sources of incompleteness for class I YSOs stems from the lack of near-infrared photometry for such objects. Multi-epoch observations are presently being acquired to complete the full-suite of scheduled VVV (K_s) photometry, which may provide photometry for a fraction of WISE targets lacking 2MASS observations, and shall invariably be utilized in concert with longer-wavelength photometry to constrain SED fits (Robitaille et al. 2007, their Fig. 3). Work likewise continues on implementing a global PSF (DAOPHOT) photometric pipeline for the VVV survey (Mauro et al. 2012, in prep). VVV images exhibit increased resolution relative to 2MASS, which is important for enabling the discernment of stellar PSFs from material endemic to the (crowded) environments surrounding YSOs (Fig. 2).

3. CONCLUSION & FUTURE RESEARCH

YSOs and (sub)clusters were identified via a hybrid $JHK_s - W_1W_2W_3W_4$ high-spectral index ($\alpha_{(LS,W,p)}$) selection scheme, namely: $(J-H) < E(J-H)/E(H-K_s)\times(H-K_s)-0.15$, $(J-K_s) < 10.5\times(W_1-W_2)-3.5$, $(J-K_s) > 4.5\times(W_1-W_2)-5.5$, $(J-K_s) > 1.6$, $(J-H) > 1$, $\alpha > -0.3$, $W_3 < 8.7$, and S/N> 5 in $W_1W_2W_3W_4$ (Fig. 1). The multiband color-color criteria were inferred from 2MASS/WISE observations for YSOs identified by Doppmann et al. (2005), Straižys & Kazlauskas (2010), Majaess et al. (2012), and Rosvick (2012, in prep). $> 30\times10^3$ YSO candidates in the preliminary WISE survey were identified. The objects delineate the Galactic plane and are constituents of giant complexes and highly-embedded (sub)clusters (Table 1, Figs. 2, 3). The impact of field contamination appears mitigated by a selection scheme that requires detections in 7-passbands, as indicated by the identification of protoclusters (Fig. 2, Table 1), the (non-isotropic) confined delineation of the Galactic plane (Fig. 3), and the rejection of the bulk of the AGB sample highlighted by Robitaille et al. (2008). The present survey is drastically incomplete since it is tied to comparatively shallow 2MASS observations (Fig. 4).

The results reaffirm the importance of the latest generation of infrared surveys (e.g., WISE) for enabling the detection of YSOs and their nascent environments (Table 1, Figs. 2, 3, see also Liu et al. 2011; Rebull et al. 2011; Koenig et al. 2012). However, significant work remains and subsequent refinement to the selection scheme (§2.1) pending the identification of biases is inevitable, especially given the relative youth of the published WISE data. Spectroscopic, deep IR photometric, and sub-mm (ALMA) follow-up observations for the cluster targets are desirable, and forthcoming.

ACKNOWLEDGEMENTS

DM is grateful to the following individuals and consortia whose efforts, encouragement, or advice enabled the research: 2MASS, WISE (D. Leisawitz), C. Bonatto, D. Turner, J. Rosvick, VVV (C. Moni Bidin, D. Minniti, J. Borissova, A-N. Chené, D. Geisler, G. Carraro), D. Balam, V. Avedisova, WEBDA (E. Paunzen), DAML (W. Dias), CDS, arXiv, NASA/IPAC ISA, and NASA ADS. This publication makes use of data products from the Wide-field Infrared Survey Explorer, which is a joint project of the University of California, Los Angeles, and the Jet Propulsion Laboratory/California Institute of Technology, funded by the National Aeronautics and Space Administration.

REFERENCES

Artigau, É., Lamontagne, R., Doyon, R., & Malo, L. 2010, procscie, 7737.
Avedisova, V. S. 2002, Astronomy Reports, 46, 193
Benjamin, R. A., Churchwell, E., Babler, B. L., et al. 2003, PASP, 115, 953
Bica, E., Dutra, C. M., & Barbuy, B. 2003, A&A, 397, 177
Bonatto, C., & Bica, E. 2011, MNRAS, 415, 2827
Bonnarel, F., Fernique, P., Bienaymé, O., et al. 2000, A&AS, 143, 33
Borissova, J., Bonatto, C., Kurtev, R., et al. 2011, A&A, 532, A131
Catelan, M., Minniti, D., Lucas, P. W., et al. 2011, RR Lyrae Stars, Metal-Poor Stars, and the Galaxy, 145
Chené, A.-N., Borissova, J., Bonatto, C., et al. 2012, A&A, in press (arXiv:1211.2801)
Churchwell, E., Babler, B. L., Meade, M. R., et al. 2009, PASP, 121, 213
Dame, T. M., Hartmann, D., & Thaddeus, P. 2001, ApJ, 547, 792
Dias, W. S., Alessi, B. S., Moitinho, A., & Lépine, J. R. D. 2002, A&A, 389, 871
Doppmann, G. W., Greene, T. P., Covey, K. R., & Lada, C. J. 2005, AJ, 130, 1145
Evans, N. J., II, Dunham, M. M., Jørgensen, J. K., et al. 2009, ApJS, 181, 321
Flaherty, K. M., Pipher, J. L., Megeath, S. T., et al. 2007, ApJ, 663, 1069
Froebrich, D., Scholz, A., & Raftery, C. L. 2007, MNRAS, 374, 399
Greene, T. P., Wilking, B. A., Andre, P., Young, E. T., & Lada, C. J. 1994, ApJ, 434, 614
Gutermuth, R. A., Megeath, S. T., Myers, P. C., et al. 2010, ApJS, 189, 352
Koenig, X. P., Leisawitz, D. T., Benford, D. J., et al. 2012, ApJ, 744, 130
Kronberger, M., Teutsch, P., Alessi, B., et al. 2006, A&A, 447, 921
Lada, C. J., & Lada, E. A. 2003, ARAA, 41, 57
Liu, W. M., Padgett, D. L., Leisawitz, D., Fajardo-Acosta, S., & Koenig, X. P. 2011, ApJL, 733, L2
Lucas, P. W., Hoare, M. G., Longmore, A., et al. 2008, MNRAS, 391, 136
Majaess, D. J., Turner, D. G., Lane, D. J., & Moncrieff, K. E. 2008, JAAVSO, 36, 90
Majaess, D. J., Turner, D. G., & Lane, D. J. 2009, MNRAS, 398, 263
Majaess, D. 2010, Acta A, 60, 55
Majaess, D., Turner, D., Moni Bidin, C., et al. 2011, ApJL, 741, L27
Majaess, D., Turner, D. G., & Gieren, W. 2012, MNRAS, 421, 1040
Mercer, E. P., Clemens, D. P., Meade, M. R., et al. 2005, ApJ, 635, 560
Minniti, D., et al. 2010, New Astronomy, 15, 433
Paunzen, E. 2008, Contributions of the Astronomical Observatory Skalnate Pleso, 38, 435
Rebull, L. M., Koenig, X. P., Padgett, D. L., et al. 2011, ApJS, 196, 4
Robitaille, T. P., Whitney, B. A., Indebetouw, R., & Wood, K. 2007, ApJS, 169, 328
Robitaille, T. P., Meade, M. R., Babler, B. L., et al. 2008, AJ, 136, 2413
Straižys, V., & Laugalys, V. 2008, Baltic Astronomy, 17, 253
Straižys, V., & Lazauskaitė, R. 2009, Baltic Astronomy, 18, 19
Straižys, V., & Kazlauskas, A. 2010, Baltic Astronomy, 19, 1
Wright, E. L., Eisenhardt, P. R. M., Mainzer, A. K., et al. 2010, AJ, 140, 1868

This 2-column preprint was prepared with the AAS LaTeX macros v5.2.

TABLE 1
(SUB)CLUSTERS

ID	J2000	size (′)	Avedisova (2002)	offset (′)	Dias et al. (2002)	offset (′)
1	00:07:21.50 +64:58:22.5	5	118.29+2.49	<1		
2	00:09:43.10 +65:20:32.0	5	118.60+2.81	<1		
3	00:10:25.80 +65:20:59.6	2 *	118.60+2.81	4		
4	00:10:53.46 +65:27:52.6	2 *	118.63+3.03	9		
5	00:10:57.67 +65:25:12.7	3 *	118.60+2.81	9		
6	00:12:16.69 +60:54:10.1	5 *	118.62-1.33	28		
7	00:14:20.66 +64:29:45.0	4	118.96+1.89	<1		
8	00:16:42.51 +64:30:20.6	3 *	119.20+1.89	<1		
9	00:21:13.23 63:19:28.5	2 *	119.56+0.65	<1		
10	00:22:57.02 +64:12:18.4	5				
11	00:23:41.38 +66:13:29.4	10	120.15+3.38	2		
12	00:24:25.30 +65:49:58.2	13	120.14+3.06	3		
13	00:26:16.15 +64:52:30.6	7	120.36+1.94	<1		
14	00:28:32.10 65:27:38.0	25	120.14+3.06	<1		
15	00:29:21.55 +64:20:02.4	3	120.54+1.56	<1		
16	00:29:53.68 +63:51:30.4	2	120.55+1.20	<1		
17	00:49:40.53 +65:24:47.4	6	122.78+2.55	2		
18	00:51:26.67 +65:47:42.7	7	123.20+2.83	<1	FSR 0516	11
19	00:58:28.52 +56:29:53.0	14	123.13-6.27	3		
20	00:58:36.69 +65:40:23.1	2 *	123.20+2.83	<1		
21	01:07:54.99 +65:20:25.7	18	124.64+2.54	<1		
22	01:08:31.65 +63:08:14.8	8	124.89+0.33	2		
23	01:10:48.27 +63:34:14.0	3 *	125.09+0.78	<1		
24	01:15:40.97 +64:46:41.4	15	125.60+2.10	<1		
25	01:21:35.52 +62:25:41.4	2 *	126.66-0.80	23		
26	01:45:40.14 +64:16:08.5	4 *	128.78+2.01	<1		
27	02:01:18.47 +67:45:33.8	4 *	129.49+5.77	<1		
28	02:17:27.02 +65:59:37.1	11				
29	02:28:07.00 +72:37:34.7	11				
30	02:44:36.37 +60:59:42.4	2 *	136.09+2.10	<1		
31	02:54:25.03 +58:10:05.2	18				
32	02:58:40.94 +62:26:41.3	18	137.07+3.00	7		
33	03:14:04.91 +58:33:06.9	12	140.64+0.67	<1		
34	03:27:31.33 +58:19:21.7	5 *	142.24+1.42	<1		
35	03:31:53.53 +60:08:13.3	5	141.68+3.23	<1		
36	03:51:36.64 +51:31:00.2	4	149.09-1.98	<1		
37	03:53:34.35 +53:36:16.0	6	148.54-0.24	8		
38	03:54:54.65 +53:44:12.9	3	148.54-0.24	9	FSR 0655	14
39	03:56:18.21 +53:52:27.0	20	148.12+0.29	<1	FSR 0655	<1
40	03:57:17.44 +54:11:07.6	5 *	148.04+0.63	<1	FSR 0654	18
41	04:03:19.02 +51:17:57.9	25	150.58-0.96	<1		
42	04:03:48.52 +51:01:05.1	2 *	150.86-1.12	<1		
43	04:05:53.47 +54:51:04.7	7	148.50+1.98	3		
44	04:07:12.43 +51:23:23.8	5 *	150.99-0.48	<1	FSR 0667	13
45	04:08:09.67 +50:31:27.4	22	151.49-1.36	13		
46	04:17:54.69 +52:49:40.6	10 *	151.32+1.99	16	Waterloo 1	6
47	04:28:28.13 +45:15:01.8	18	158.48-2.22	23		
48	04:36:32.11 +51:13:53.4	15	154.35+2.61	2		
49	04:40:26.46 +60:27:40.5	10	147.77+9.17	<1		
50	04:45:29.66 +41:58:33.2	17	162.28-2.34	<1	FSR 0721	10
51	04:45:45.50 +42:02:05.0	16	162.28-2.34	5	FSR 0717	7
52	04:59:11.78 +47:51:19.6	7	159.16+3.30	9	FSR 0696	10
53	05:00:23.19 +39:56:33.7	14 *				
54	05:16:48.64 +37:01:15.6	8 *	169.95-0.59	<1		
55	05:19:01.46 +36:47:33.4	7 *	170.67-0.27	18		
56	05:21:07.27 +36:39:45.1	6 *	170.67-0.27	<1		
57	05:21:53.02 +36:38:51.8	4 *	170.80+0.00	<1		
58	05:25:51.98 +34:52:30.0	14			FSR 0775	6
59	05:27:13.61 +38:32:10.8	50	169.85+1.92	2		
60	05:37:23.23 +27:46:20.9	13	180.03-2.15	<1		
61	05:38:23.00 +27:26:59.0	4	180.40-2.13	<1		
62	05:39:10.00 +27:32:13.2	4 *	180.40-2.13	12		
63	05:40:19.60 +23:52:02.5	10	183.70-3.64	2		
64	05:42:46.26 -09:48:03.9	12	210.76-19.61	12		
65	05:49:44.39 +27:06:29.6	14	182.36+0.18	19		
66	05:51:29.90 +27:28:50.0	8	181.92+0.36	<1	Dutra Bica 83	9
67	05:52:03.29 +27:23:55.6	5	182.36+0.18	<1	Dutra Bica 83	<1

TABLE 1—*Continued*

ID	J2000	size (′)	Avedisova (2002)	offset (′)	Dias et al. (2002)	offset (′)
68	05:52:12.90 +26:59:33.0	22	182.36+0.18	<1		
69	05:58:13.65 +16:33:33.5	15	192.16-3.83	2		
70	06:00:58.09 -09:54:12.3	40				
71	06:02:01.76 +20:08:44.7	6 *	189.21-1.06	19		
72	06:02:08.70 +20:27:47.8	9 *	189.21-1.06	<1		
73	06:02:16.88 -09:06:28.8	17				
74	06:02:45.97 -09:43:16.8	20	216.31-15.05	9		
75	06:09:44.27 +21:07:03.7	3	189.68+0.72	12		
76	06:10:53.58 +14:09:41.3	6 *	196.07-3.43	27	FSR 0939	13
77	06:12:05.34 +20:15:12.6	5	190.04+0.49	18		
78	06:13:35.82 +15:57:39.6	4	193.69-1.05	22		
79	06:27:51.82 +05:31:40.0	8	206.30-2.11	2		
80	06:32:32.03 +10:19:56.0	15	201.60+0.53	<1		
81	06:33:15.80 +02:30:22.0	3	208.51-3.21	<1		
82	06:36:39.88 +05:36:01.7	3 *	206.26-0.71	<1		
83	06:58:53.26 -07:45:00.3	2 *	220.80-1.72	8		
84	07:00:34.54 -09:11:52.0	4 *	221.85-2.02	<1	Ivanov 4	20
85	07:03:26.34 -09:19:56.3	40	221.85-2.02	19		
86	07:18:30.50 -18:22:15.0	11	231.96-2.06	5	ESO 559 02	15
87	07:19:35.87 -17:49:10.4	50	231.96-2.06	<1		
88	07:24:07.03 -25:53:55.9	6	237.25-6.50	2		
89	07:24:37.71 -24:34:59.4	5	237.25-6.50	<1	Ivanov 6	6
90	07:24:44.88 -24:29:34.5	5	237.25-6.50	<1	Ivanov 6	11
91	07:33:15.92 -22:09:19.9	14	237.26-1.28	<1		
92	07:34:22.54 -22:37:01.1	9 *	238.77-1.61	15		
93	07:50:14.40 -33:37:07.8	25	248.97-3.61	10		
94	07:51:54.59 -33:14:04.5	8	248.96-3.21	<1		
95	08:17:52.55 -35:52:47.6	3 *	254.05-0.10	<1		
96	08:18:14.71 -36:03:53.3	3 *	254.05-0.10	<1		
97	08:19:10.56 -41:52:04.6	3 *				
98	08:20:31.81 -41:51:47.2	3 *	259.28-2.61	26		
99	08:21:44.62 -42:04:55.4	10	259.61-2.70	17		
100	08:22:22.39 -41:36:14.4	2 *	259.28-2.61	<1		
101	08:22:48.83 -41:37:09.8	2 *	259.28-2.61	5		
102	08:22:51.06 -41:42:13.7	2 *	259.28-2.61	8		
103	08:23:00.09 -41:55:44.9	9	259.61-2.70	<1		
104	08:23:15.31 -41:46:05.7	6 *	259.61-2.70	10		
105	08:24:00.40 -42:24:15.0	4 *	260.18-3.14	19		
106	08:24:41.14 -40:59:57.9	7	259.29-1.95	16	ESO 312 03	18
107	08:29:13.96 -41:10:47.7	16	259.63-1.30	<1		
108	08:34:20.73 -38:40:28.6	6 *				
109	09:03:43.11 -50:28:31.7	13				
110	09:07:38.57 -50:41:40.2	8 *	271.22-1.77	22		
111	09:16:10.38 -50:02:59.0	4 *	271.59-0.53	12	Pismis 11	3
112	09:18:19.45 -48:26:44.1	20	270.82+0.69	<1		
113	09:19:01.86 -46:14:10.1	2 *				
114	09:22:20.28 -48:03:58.6	4 *	271.01+1.39	<1		
115	09:22:41.44 -48:10:07.1	4 *	271.01+1.39	2		
116	10:03:40.11 -57:26:38.2	7	281.84-1.59	<1		
117	10:05:42.66 -57:56:14.9	12	282.21-2.00	5		
118	10:07:30.62 -60:02:38.5	2 *	283.74-3.41	<1	Trumpler 12	17
119	10:09:27.46 -58:38:51.0	10	283.55-2.27	24		
120	10:10:38.80 -57:45:32.0	13	282.81-1.34	<1		
121	10:11:51.12 -58:53:12.6	12 *	283.55-2.27	7		
122	10:12:19.50 -57:34:08.0	10 *	283.55-0.98	16		
123	10:20:56.75 -59:41:06.1	40	285.04-2.00	11	SAI 113	17
124	10:26:36.08 -56:33:34.2	18 *				
125	10:30:33.41 -58:53:52.0	5	285.59-0.85	<1		
126	10:32:36.99 -59:38:48.1	10	286.40-1.35	11		
127	10:33:56.48 -59:43:58.0	13	286.40-1.35	<1		
128	10:56:07.77 -60:29:15.9	7 *	289.07-0.36	10	ASCC 63	5
129	10:56:26.88 -60:07:42.5	22	289.07-0.36	<1	ASCC 63	17
130	10:56:59.22 -58:36:44.0	9				
131	10:57:41.59 -60:45:45.8	6	289.41-0.68	10		
132	10:58:05.23 -58:49:32.3	14			Hogg 9	14
133	10:58:42.73 -61:11:14.9	4 *	289.77-1.30	<1		
134	10:59:17.09 -60:34:38.9	7	289.58-0.64	<1		

TABLE 1—*Continued*

ID	J2000	size (′)	Avedisova (2002)	offset (′)	Dias et al. (2002)	offset (′)
135	10:59:35.38 -59:00:01.8	4 *			Hogg 9	10
136	11:01:00.13 -58:19:18.7	2 *				
137	11:01:04.94 -60:51:01.5	50	289.88-0.75	<1		
138	11:20:11.34 -62:01:51.8	6 *	292.92-0.90	29		
139	11:24:48.85 -62:13:25.4	4	293.03-1.03	<1		
140	11:25:39.64 -62:10:43.8	8	293.09-0.97	<1		
141	11:27:29.08 -62:22:55.2	10 *	293.09-0.97	12		
142	11:32:40.59 -62:21:15.7	20	293.82-0.76	2		
143	11:36:44.16 -65:48:45.0	10 *				
144	11:54:46.89 -63:07:39.6	20	296.59-0.97	<1		
145	11:54:59.78 -62:36:25.5	5				
146	11:58:59.03 -63:37:15.9	20	296.89-1.31	15		
147	12:19:55.50 -62:55:04.0	8	299.30-0.31	<1		
148	12:19:57.68 -63:45:14.1	7 *	299.46-1.09	<1		
149	12:41:10.10 -62:33:48.8	3 *	302.13+0.29	23		
150	12:54:51.86 -61:02:53.7	9				
151	12:57:22.68 -61:31:34.2	5	303.28+1.32	22		
152	13:00:54.34 -62:33:46.1	20				
153	14:09:51.38 -59:45:58.6	5 *				
154	14:12:11.33 -60:56:42.0	6 *	312.60+0.05	21		
155	14:14:13.65 -61:15:44.2	7	312.60+0.05	7		
156	14:14:29.43 -61:12:41.6	3 *	312.60+0.05	10		
157	14:22:03.62 -61:04:04.1	3 *	313.67-0.12	<1		
158	14:22:32.41 -61:08:22.6	5 *	313.67-0.12	<1		
159	15:00:33.05 -63:13:08.7	12	314.80-5.20	4		
160	15:03:26.41 -63:23:15.1	6 *	314.80-5.20	24		
161	15:19:36.70 -57:19:02.5	14	321.65-0.03	16		
162	15:26:51.68 -56:29:13.5	4 *	323.46+0.08	15		
163	15:29:53.36 -56:35:19.7	30	323.46-0.08	6		
164	15:31:35.89 -56:11:33.5	20	323.93+0.01	<1		
165	15:35:16.14 -55:39:31.8	13 *	324.71+0.34	11		
166	15:53:21.08 -55:14:51.6	4 *	326.86-1.04	5		
167	15:58:02.97 -53:57:24.1	18	328.18-0.59	<1		
168	15:59:35.20 -52:24:21.6	4 *	329.46+0.51	<1		
169	15:59:58.46 -51:37:44.8	10 *	330.07+1.06	4		
170	16:00:51.55 -51:42:40.3	5 *	330.07+1.06	9		
171	16:23:27.20 -49:28:56.8	9 *	334.17+0.07	<1		
172	16:29:02.12 -48:59:33.6	7 *	335.06-0.42	13		
173	16:50:50.75 -46:10:43.8	5	339.72-1.12	<1		
174	17:00:54.30 -42:19:10.0	3 *	343.72-0.22	11		
175	17:03:25.71 -42:36:05.8	7	343.93-0.64	<1		
176	17:04:09.49 -42:28:12.1	5 *	344.23-0.59	<1		
177	17:04:14.39 -42:19:57.6	12	344.23-0.59	<1		
178	17:11:21.12 -27:25:00.4	9	357.08+7.19	<1		
179	17:25:03.87 -37:59:13.0	10 *	350.01-1.34	5	Ruprecht 123	20
180	17:28:18.91 -35:04:11.4	4 *	352.87-0.20	<1		
181	17:30:18.11 -33:09:18.8	19	354.66+0.47	2		
182	17:31:15.50 -33:52:24.7	12	354.20-0.05	<1		
183	17:31:20.10 -33:18:35.4	7	354.67+0.25	<1		
184	17:39:17.36 -31:08:46.1	5 *	357.49-0.04	5		
185	17:41:23.84 -30:43:35.9	4 *	357.99-0.17	<1		
186	17:54:33.00 -25:52:05.3	7	3.66-0.11	<1		
187	18:06:14.33 -20:31:50.1	10	9.62+0.19	<1		
188	18:07:20.28 -21:52:34.5	5 *	8.72-0.51	<1		
189	18:08:18.27 -20:16:02.6	12	10.08-0.09	<1		
190	18:08:19.78 -22:04:32.1	4 *	8.72-0.51	<1	ASCC 93	11
191	18:08:38.58 -19:52:30.5	5 *	10.45+0.02	<1		
192	18:09:01.23 -20:05:06.7	18	10.30-0.15	<1		
193	18:09:09.73 -19:28:38.1	20	10.87+0.09	<1		
194	18:10:28.02 -19:57:09.9	16	10.60-0.39	<1		
195	18:16:52.12 -18:41:00.1	10	12.46-1.07	<1	Turner 4	4
196	18:28:23.69 -07:41:01.7	8 *	23.45+1.55	<1		
197	18:59:44.45 +01:01:23.7	2 *	35.20-1.75	<1		
198	19:05:14.43 01:37:17.0	9				
199	19:34:45.73 +19:31:52.7	3 *	55.16-0.30	<1		
200	19:34:56.61 +19:14:55.1	6 *	55.16-0.30	17		
201	19:36:13.21 +20:23:30.4	15	56.25-0.17	10	FSR 0142	18

TABLE 1—*Continued*

ID	J2000	size (′)	Avedisova (2002)	offset (′)	Dias et al. (2002)	offset (′)
202	20:05:45.46 +23:25:46.9	5 *	62.20-4.53	<1		
203	20:11:29.49 +40:13:40.6	3 *	76.88+3.28	17		
204	20:19:48.51 +36:45:50.7	6 *	75.22+0.01	20		
205	20:20:35.73 +36:50:49.0	3 *	75.22+0.01	11		
206	20:23:34.49 +36:39:01.1	25	75.35-0.43	<1		
207	20:24:12.98 +35:52:20.6	7 *	74.79-0.96	<1		
208	20:24:39.08 +36:05:45.6	5 *	74.79-0.96	14		
209	20:37:21.40 +47:14:04.5	2 *	85.41+3.74	<1		
210	20:42:39.24 +48:53:38.3	9	87.24+4.05	2		
211	21:13:15.44 +46:22:09.0	5 *	88.72-1.50	<1		
212	21:49:40.33 +56:54:40.8	1 *	100.01+2.36	<1		
213	22:07:56.62 +59:46:39.0	25	103.55+3.12	8		
214	22:30:00.08 +61:32:55.0	4	106.90+3.16	<1	Teutsch 76	10
215	22:49:34.51 +59:56:08.6	6	108.20+0.58	<1		
216	22:52:42.46 +60:00:04.9	4 *	108.75+0.25	<1		
217	22:59:43.08 +62:46:43.6	3 *	110.15+2.61	<1	FSR 0413	11
218	23:01:22.54 +64:17:21.6	2 *	111.34+3.92	<1		
219	23:17:52.60 +58:05:10.0	20 *	110.78-2.86	17		
220	23:18:42.30 +57:44:50.5	30	110.78-2.86	4		
221	23:25:51.86 +64:07:47.0	13	113.77+2.79	<1		
222	23:29:07.07 +59:34:19.7	7	111.73+0.04	27		
223	23:30:08.12 +59:25:29.8	9 *	111.73+0.04	27		
224	23:39:17.80 +61:59:14.0	6	114.61+0.22	4		
225	23:39:47.91 +61:55:41.9	12	114.61+0.22	<1		
226	23:46:00.23 +59:07:16.8	2 *	114.61-2.69	<1	FSR 0443	19
227	23:47:18.81 +60:28:03.2	13 *	115.11-1.44	<1		
228	23:50:48.85 +63:41:38.8	8				
229	23:51:08.19 +63:53:07.8	7				